First Experimental Campaign on SMOLA Helical Mirror*)

Anton V. SUDNIKOV[1,2)], Aleksey D. BEKLEMISHEV[1,2)], Vladimir V. POSTUPAEV[1,2)], Ivan A. IVANOV[1,2)], Anna A. INZHEVATKINA[2)], Vladislav F. SKLYAROV[1,2)], Aleksandr V. BURDAKOV[1,3)], Konstantin N. KUKLIN[1)], Andrey F. ROVENSKIKH[1)] and Nikita A. MELNIKOV[1)]

[1)]*Budker Institute of Nuclear Physics, 11 Acad. Lavrentiev av., Novosibirsk, Russia*
[2)]*Novosibirsk State University, 2 Pirogov str., Novosibirsk, Russia*
[3)]*Novosibirsk State Technical University, 20 Karl Marx av., Novosibirsk, Russia*

(Received 14 September 2018 / Accepted 16 December 2018)

Experimental evidence of the plasma flow suppression by the helical magnetic mirror is presented. Reported experiments were done during the first plasma campaign in the SMOLA helical mirror device at self-consistent floating potentials of all in-vessel electrodes and at minimal magnetic fields suitable for confinement regime. The experimental results are consistent with two main theory predictions for the helical mirror confinement: a reduction of the axial plasma flow and the inward particle pinch. The helical mirror technology can dramatically improve fusion reactor prospects of open magnetic configurations.

Keywords: magnetic confinement, controlled fusion, open trap, dynamic multimirror confinement, moving magnetic mirrors, helical mirror

DOI: 10.1585/pfr.14.2402023

1. Introduction

Advances plasma confinement in open magnetic mirrors features high relative pressure ($\beta \approx 60\%$), mean energy of hot ions of 12 keV and the electron temperature up to 0.9 keV in quasistationary regime [1–3]. At the same time, the mirror ratio in a simple open trap is limited by the achievable magnetic field and is supposed to be 15 - 20 in neutron source concepts [4]. Higher fusion gain in linear plasma devices is possible with improved longitudinal confinement [5]. Existing method of multiple-mirror suppression of the axial heat flux combined with gas-dynamic central cell [6, 7] can provide effective mirror ratios of the order of 100, which gives feasible fusion gain appropriate for hybrid systems.

Recently, a new method of active plasma flow suppression in a helical magnetic field was proposed [8, 9]. That proposal renewed the idea of a plasma flow control with moving magnetic mirrors [10]. Recent analysis in [11] have shown that the modulation of the guiding magnetic field travelling in the laboratory reference frame may be achievable, but presumably restricts the usage of the superconducting magnetic system due to the mechanical stresses and coil quenching. Therefore, an emulation of the moving magnetic mirrors by the stationary magnetic field is still of sufficient interest.

Plasma rotation in $\boldsymbol{E} \times \boldsymbol{B}$ fields similar to vortex confinement [12] can be utilized to create periodical variations of helicoidal magnetic field moving upstream in plasma's frame of reference. These variations transfer momentum to trapped particles [13] and lead to plasma pumping towards the central trap. Theory predicts exponential dependence of the flow suppression on the magnetic structure length, that is more favorable then the power dependence in passive magnetic systems. Plasma biasing or natural ambipolar potential can drive the rotation. The first case also leads to plasma pinching [14]. Plasma acceleration can also be achieved [15].

Concept exploration device SMOLA with a helical mirror started operation in the end of 2017 in BINP [16]. The main parameters were discussed in [9].

Here we report the experimental observation of the rotating plasma flow suppression in a helical magnetic mirror from the first plasma campaign. The aim of the first experiments was to prove the concept itself, regardless of the efficiency. Some of subsystems were not installed yet or was operating in interim configurations. The layout of the device and the positions of the diagnostics are shown in Fig. 1.

2. Experimental Setup and Parameters

In these experiments, the influence of the magnetic configuration on the plasma stream parameters was studied. Hydrogen plasma with the density $\sim 10^{19}$ m^{-3} and temperature 2 - 5 eV was generated by the plasma gun, based on the design of [17]. Ionization is performed by the electrons emitted from heated LaB_6 cathode. Potentials of the anode and cathode are independent and magnetically insu-

author's e-mail: A.V.Sudnikov@inp.nsk.su

*) This article is based on the presentation at the 12th International Conference on Open Magnetic Systems for Plasma Confinement (OS2018).

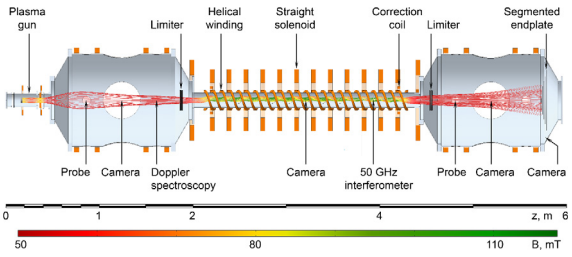

Fig. 1 (Color online) Layout of the SMOLA helical mirror. Main systems and diagnostics are shown. Color scale indicates the magnetic field strength at the plasma boundary; all magnetic fields below 50 mT are shown in red.

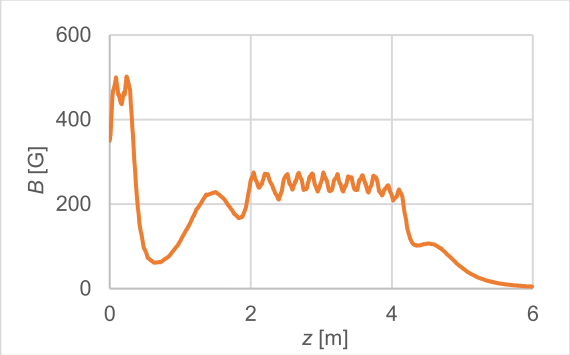

Fig. 2 Axial magnetic field (low-field regime) in SMOLA helical mirror with the first-stage solenoidal winding.

lated by the guide field 0.06 - 0.2 T of each other and of the grounded vacuum chamber (Fig. 2). The plasma source always operated at the same parameters, providing the same plasma flow.

The gun-generated plasma can be trapped in the entrance expander between the high-field region of the plasma gun and the helical section.

Plasma passed along the 2.5-m-long transport section with helical magnetic corrugation The magnetic system of the transport section consisted of two separately-powered windings, which created the straight and the helical components of the magnetic field. In the first plasma campaign, we used a temporary solenoidal winding instead of that shown in Fig. 1. It provided lower magnetic field (up to 0.04 T) and had significant parasitic field strength modulation along the axis. After the transport section, the plasma stream passed to the exit magnetic expander featuring radially-segmented electrically-insulated endplates.

The plasma rotation was driven by the radial electric field of the plasma gun; external sources were not used to form the particular predefined profile of the radial electric field. Electric field of the gun corresponds to the negative charge on the plasma axis.

Significant dimensionless parameters were the following:

— pitch of the helical field to the ion mean free path $h/\lambda \sim 0.5$ - 1,

— mean corrugation $R_{mean} \sim 1.5$ - 2,

— ion gyroradius to the plasma radius $\rho/r \sim 0.1$,

— longitudinal velocity of the magnetic corrugation, in the plasma's frame of reference to the ion thermal velocity $v_z/v_T \sim 1$.

The magnetic corrugations moved oppositely the plasma flow. Two significant effects were expected in this case: flow suppression at the plasma periphery with higher magnetic corrugation along the field line, and radial plasma pinchng [14]. Both of these effects lead to the radial contraction of the discharge.

An experiment with the opposite direction of the rotation was also performed to exclude an effect of the static multiple mirror confinement. Due to $v_z/v_{Ti} \sim 1$, the helical field component should not have influenced the flow significantly.

The plasma density was measured by the set of movable Langmuir probes and the 50 GHz interferometer. The plasma rotation velocity was calculated from the spatial distribution of the Doppler shift of the Hα emission, like in [18]. Spectrometer sightline was inclined at ~45° to the magnetic axis. In the axially symmetric case uniform shift of the spectral line corresponds to the exhaust velocity and its tilt is proportional to the angular rotation speed. Monitoring of the impurities was based on the visible light spectroscopy. Several cameras, including the fast video at 5000 fps, were used for monitoring the plasma shape and displacements.

3. Results and Discussion

The full discharge duration was 0.19 s; it had four phases that can be seen from the waveforms shown in Fig. 3. During the ramp-up phase (0 - 0.02 s), the discharge current rises to its nominal value and the plasma fills the entire machine. In this phase, the potential is due to ~ 200 eV electrons emitted from the cathode. The second phase (0.02 - 0.05 s for the straight-field experiments and 0.02 - 0.06 for the helical field ones) corresponds to formation of the stationary profiles of the potential and density; the plasma rotational velocities are maximal during this period. At the end of this phase, the plasma density in the exit expander rises to its maximal value. During the third phase (0.06 - 0.1 s) the plasma column is fully formed in the entire length of the device, its rotational velocity decreases but stays significantly non-zero. During the fourth phase (> 0.1 s), the plasma rotation decreases to non-measurable values. This was caused presumably by the steady growth of neutral gas pressure, which leads to a friction-like force due to charge-exchange processes.

Main discharge parameters (Figs. 3(a), 3(b)), plasma density (Fig. 3(e)), its shape, and visible spectrum of the plasma before helical mirror do not depend on the presence of the helical component of the magnetic field. Density profile in the entrance expander also does not significantly

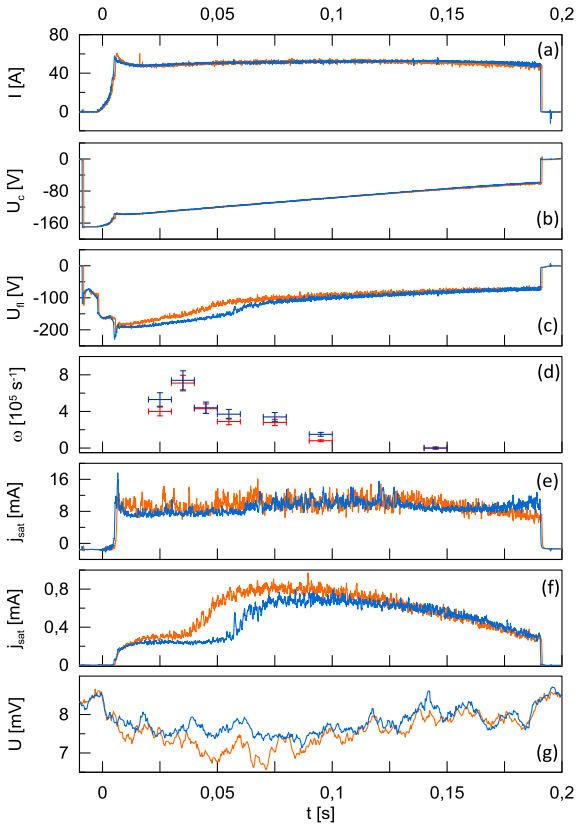

Fig. 3 (Color online) Typical plasma parameters in shots without (SM1936, red color) and with (SM1937, blue color) the helical corrugation. From top to bottom: (a) the plasma gun current, (b) the voltage between the cathode and the anode, (c) the potential of the central endplate, (d) the rotation velocity in the entrance tank, (e) the ion saturation current of the Langmuir probe at the axis in the entrance tank at $z = 0.4$ m, (f) the ion saturation current of the Langmuir probe at the axis in the entrance tank at $z = 4.34$ m, (g) the raw signal of the 50 GHz interferometer at $z = 3.48$ m. Time $t = 0$ s corresponds to the discharge initiation by the hydrogen flow start.

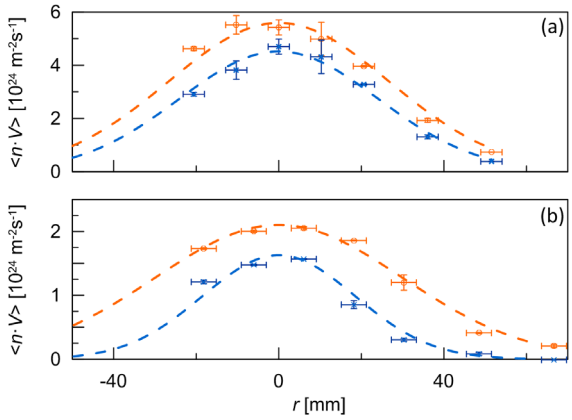

Fig. 4 (Color online) Particle flux density profiles averaged for 0.07 - 0.1 s interval before (a) and after (b) the transport section are shown for configurations with (blue crosses) and without (red circles) the helical field corrugation. Smooth lines of corresponding colors are Gaussian fits. The radial scale was recalculated for a magnetic flux tube coordinates at the position of the interferometer.

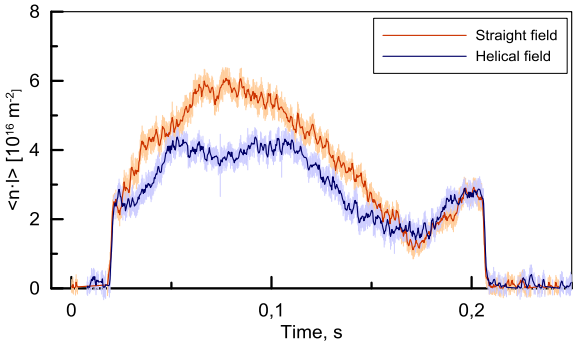

Fig. 5 (Color online) Line averaged plasma densities at $z = 3.48$ m with (blue line) and without (red line) the helical corrugation.

change by the configuration of the magnetic field in helical plug (Fig. 4(a)).

At the same time, direct comparison of the experimental signals show significant difference between plasma parameters at the exit from the helical section with and without helical field (Figs. 3(c), 3(f), 3(g)) in quasi-stationary phase. Difference become negligible when rotation velocity drops to zero. We observed minor changes at the axis and significant decrease of the density in the periphery. This is consistent with theory predictions of the helical mirror confinement and inwards pinching. The plasma stream width at the half-maximum at the exit from the helical mirror was 70 ± 5 mm in the solenoidal configuration, whereas it decreased to 43 ± 8 mm with the helical field in the deceleration regime – see Fig. 4 (b). Changes of the plasma radius in the entrance tank were within the measurement accuracy (73 ± 4 mm vs. 66 ± 5 mm), albeit this difference is in the correct direction. One can note that the plasma radius in the magnetic flux coordinates increased by $\approx 13\%$ due to the transversal trasnsport in the solenoidal configuration; on the contrary, the plasma radius decreased in the helical field by $\approx 30\%$.

The interferometry data was averaged over ~25 discharges in each regime. Line averaged plasma density at the exit is suppressed by the factor of 1.25 compared to the regime with straight field lines (Fig. 5).

In the series with the reversal of the magnetic field direction in all coils, the magnetic mirrors moved with the plasma flow at approximately the same velocity. No influence of the helical field was expected for our set of experimental paremeters, exactly as we got from the experiment.

Experiments in the first plasma campaign evidently demonstrated the flow suppression with the helical mirror in the flow reduction mode.

Experiments in the first plasma campaign in the

SMOLA helical mirror trap evidently demonstrated the plasma flow suppression with activation of the helical winding in the flow reduction mode. The reported experiments were done at self-consistent floating potentials of all in-vessel electrodes without the controlled biasing (except for the plasma gun) and with the first-stage solenoidal winding, which has a large modulation of the magnetic field along the axis. In the current configuration, the axial modulation of the solenoidal magnetic field introduces some effects of the multiple-mirror confinement, which may slow down the plasma flow even without the helical component. This complicates the direct comparison of the reported experiment with theory predictions.

Even at these conditions, we observed two main effects predicted by theory: the decrease of the plasma flow through the transport section and its radial contraction. We expect stronger and more controllable effect in the final configuration of SMOLA. Integration of helical mirror sections into the existing GDMT project of the next-generation open trap should improve its equivalent fusion gain factor from $Q_{\mathrm{DT}} = 0.25$ in the original project [5] to the approximately unity in the revised configuration that is currently under discussion in BINP. The required magnetic technologies for a reactor-grade system are less demanding than that already suggested for stellarator-based fusion plants.

This work was funded by Russian Science Foundation (project 18-72-10080).

[1] T.C. Simonen *et al.*, J. Fusion Energy **29**, 558 (2010).
[2] P.A. Bagryansky *et al.*, Nucl. Fusion **55**, 053009 (2015).
[3] A.A. Ivanov and V.V. Prikhodko, Physics-Uspekhi **60** (5), 509 (2017).
[4] A.V. Anikeev *et al.*, Materials **8**, 8452 (2015).
[5] A.D. Beklemishev *et al.*, Fusion Sci. Technol. **63** (No. 1T), 46 (2013).
[6] V.V. Postupaev *et al.*, Nucl. Fusion **57**, 036012 (2017).
[7] A.V. Burdakov and V.V. Postupaev, AIP Conf. Proc. **1771**, 080002 (2016).
[8] A.D. Beklemishev, Fusion Sci. Technol. **63** (No. 1T), 355 (2013).
[9] V.V. Postupaev *et al.*, Fusion Eng. Des. **106**, 29 (May 2016).
[10] G.I. Budker, V.V. Mironov and D.D. Ryutov, "Gas dynamics of a dense plasma in a corrugated magnetic field." In Collection of papers (1982).
[11] Ilan Be'ery *et al.*, Plasma Phys. Control. Fusion, in press (2018). https://doi.org/10.1088/1361-6587/aadd69
[12] A.D. Beklemishev *et al.*, Fusion Sci. Technol. **57**, 351 (2010).
[13] A. Burdakov *et al.*, Fusion Sci. Technol. **51** (No. 2T), 106 (2007).
[14] A.D. Beklemishev, AIP Conf. Proc. **1771**, 040006 (2016).
[15] A.D. Beklemishev, Phys. Plasmas **22**, Iss.10, 103506 (2015).
[16] A.V. Sudnikov, Fusion Eng. Des. **122**, 85 (2017).
[17] V.I. Davydenko, A.A. Ivanov and G.I. Shul'zhenko, Plasma Phys. Rep. **41** (11), 930 (2015).
[18] I.A. Ivanov *et al.*, Instrum. Exp. Tech. **59** (2), 262 (2016). https://doi.org/10.1134/s0020441216020214